Combination of CG methylation and Chromomethylase 2-mediated RdDM-independent CHH methylation is required for chromosome-specific rRNA gene silencing

Navinchandra V. Puppala[1†], Ramya Tammineni[2†], Gargi P. Saradadevi[3], and Gireesha Mohannath[2*]

[1]Institute for Developmental Biology and Neurobiology, Johannes Gutenberg University Mainz, Biozentrum I, Mainz, Germany

[2]Department of Biological Sciences, Birla Institute of Technology and Science-Pilani, Hyderabad campus, Hyderabad, Telangana, India.

[3]Stem Cells Division, SKAN Research Trust, St. John's Research Institute, Bengaluru, Karnataka, India

[†] These authors contributed equally to this work

Corresponding author:
Email: gireesha@hyderabad.bits-pilani.ac.in

Abstract

Arabidopsis thaliana has two nucleolus organizer regions (NORs), consisting of long tandem arrays of 45S rRNA genes on chromosomes 2 (*NOR2*) and 4 (*NOR4*). The rRNA gene subtypes mapping to *NOR2* are mostly silenced during development, whereas most of those mapping to *NOR4* are active. Cytosine methylation of promoters plays a significant role in rRNA gene silencing, but recent findings demonstrate that gene body methylation also play a key role in gene silencing. Previous studies have demonstrated that CG methylation plays a role in rRNA gene silencing. However, it remains to be determined whether Chromomethylase 2 (CMT2)-mediated, RdDM-independent CHH methylation plays any role in rRNA gene silencing. To find out the relative importance of cytosine methylation in each of the sequence contexts (CG, CHG, and CHH, where H=A, T, or C), we studied multiple DNA methylation-deficient *Arabidopsis* mutants. Primarily, we show that the mutants that displayed higher losses of CG or CHH methylation at rDNA loci, display higher degrees of *NOR2* rRNA gene silencing disruption. Using whole genome bisulfite sequencing data, we show that the loss of RdDM-independent CMT2, not the loss of RdDM-dependent DRM2, erases most of the CHH methylation at rDNA loci, while retaining CG methylation levels comparable to those of wild-type Col-0, demonstrating the sufficiency of CHH methylation loss for releasing rRNA gene silencing. Analysis of *Arabidopsis* and tomato NOR sequences revealed that in 45S rRNA gene sequences, cytosines mostly occur in the CHH context, followed by CG and the lowest being in CHG contexts. The predominance of CHH sites is even more pronounced when the rRNA gene promoter and spacer promoter(s) are considered (0-7% CG, 14-25% CHG, and 79-80% CHH), suggesting a mechanism to explain the stronger disruption of *NOR2* gene silencing in mutants that display higher losses of CHH methylation. Our data also reveal a role for gene body methylation in rRNA gene silencing. We show that *NOR2* genes are relatively hypermethylated compared to *NOR4*, consistent with findings from recent studies. By contrast, human rRNA genes have more CG sites than CHH and CHG, correlating with the evolutionary loss of CMTs in mammals. CMTs are plant-specific, which primarily methylate CHG and CHH sites. Our data define a critical role for CMT2-mediated RdDM-independent CHH methylation, in combination with MET1-mediated CG methylation, in rRNA gene silencing, which is entirely mediated by CG methylation in mammals.

Key words:

Ribosomal RNA (rRNA), rDNA promoter, Nucleolus organizer region (NOR), Gene silencing, DNA cytosine methylation, Chromomethylase 2 (CMT2), DDM1, MET1

Introduction

In eukaryotes, hundreds to thousands of 45S ribosomal RNA (rRNA) genes are arranged as tandem repeats at chromosomal loci known as nucleolus organizer regions (NORs) (Gerbi, 1986, Long and Dawid, 1980, Viktorovskaya and Schneider, 2015). RNA polymerase I (Pol I) transcribes rRNA genes to produce 45S pre-rRNA transcripts that are then processed into 18S, 5.8S, and 25-28S rRNAs that comprise the catalytic core of ribosomes, which synthesize proteins in cells (Saradadevi et al., 2020, Turowski and Tollervey, 2015, Viktorovskaya and Schneider, 2015). Although eukaryotic genomes contain many rRNA genes, not all of them are transcribed at all times. Instead, the number of genes transcribed varies during development, dictated by the developmental stage-specific need for ribosomes and protein synthesis (Grummt, 2013, Hannan et al., 2013, Moss et al., 2007). rRNA 'dosage control' involves selective gene silencing rather than selective gene activation (Chen and Pikaard, 1997, Pikaard et al., 2023). In *Arabidopsis thaliana*, rRNA genes are clustered within two NORs located at shorter arms of chromosomes 2 (*NOR2,* which spans ~ 5.9 Mb) and 4 (*NOR4,* which spans ~ 3.9 Mb) (Copenhaver et al., 1995, Copenhaver and Pikaard, 1996b, Copenhaver and Pikaard, 1996a, Fultz et al., 2023). Previous findings in *A. thaliana* demonstrated that the selective silencing of rRNA genes is determined by their chromosomal location, not rRNA gene sequence variation (Chandrasekhara et al., 2016, Mohannath et al., 2016). During development, rRNA genes located on *NOR2* are selectively silenced while most of those on *NOR4* remain active (Chandrasekhara et al., 2016, Mohannath et al., 2016).

Transcriptional gene silencing in eukaryotes often involves cytosine methylation and chromatin condensation (Rhee et al., 2002, Zhang et al., 2006, Zilberman et al., 2007). Recent findings have demonstrated that in addition to gene promoter methylation, gene body methylation also plays a role in gene silencing (Lee et al., 2023a, Shahzad et al., 2025, Williams et al., 2023). Although cytosine methylation has been known to play a role in rRNA gene silencing (Costa-Nunes et al., 2010, Pontvianne et al., 2013, Preuss et al., 2008), the relative role of cytosine methylation in all three sequence contexts (CG, CHG, and CHH, where H=A, C, or T) in selectively silencing *NOR2* rRNA genes remains unclear. In plants, cytosine methylation is deposited by several DNA methyltransferases belonging to different families. *METHYLTRANSFERASE 1* (*MET1*) and *CHROMOMETHYLASE 3* (*CMT3*) mediate virtually all *Arabidopsis* CG and CHG methylation, respectively (Cokus et al., 2008, Lister et al., 2008, Zemach et al., 2013). CHH methylation is directed by small RNAs and mediated by *DOMAINS REARRANGED METHYLTRANSFERASE 2* (*DRM2*) via the RNA-directed DNA methylation (RdDM) pathway, but also by *CHROMOMETHYLASE 2* (*CMT2*) independently of RdDM (Zemach et al., 2013, Law and Jacobsen, 2010, Rymen et al., 2020, Sasaki et al., 2019). *CMT2* and *CMT3* belong to a group of plant-specific chromomethylases (Bewick et al.,

2017). In addition to the aforementioned DNA methyltransferases, *DECREASE IN DNA METHYLATION 1* (*DDM1*), a SWI2/SNF2 family chromatin remodeler, acts as a master regulator of DNA methylation (Brzeski and Jerzmanowski, 2003, Lee et al., 2023b, Osakabe et al., 2021). Loss of DDM1 results in genome-wide demethylation at 70% of methylated cytosines in all three sequence contexts (CG, CHG, and CHH) (Jeddeloh et al., 1999, Vongs et al., 1993, Zemach et al., 2013). Recent findings have demonstrated that DDM1-mediated gene body methylation also contributes to silencing of genes involved in defense response (Lee et al., 2023a).

An earlier study investigated the effects of *drm2*, *cmt3,* and *met1* mutants on rRNA gene silencing (Pontvianne et al., 2013). However, these mutants predominantly exhibit a loss of CG or CHG methylation accompanied by a minimal to modest loss of CHH methylation (Cokus et al., 2008, Zemach et al., 2013). Among these, *met1* mutants displayed the maximum disruption of *NOR2* gene silencing, which is attributed mainly to the loss of CG methylation in these mutants. In this study, we analysed *ddm1* and *cmt2* mutants, along with the three previously studied (*drm2*, *cmt3*, and *met1*) DNA methylation-deficient mutants to compare the relative effects of differential loss of CG, CHG, and CHH methylation on the disruption of chromosome-specific *NOR2* rRNA gene silencing. In this mutant panel, we show higher disruption of *NOR2* rRNA gene silencing in the mutants that displayed maximum loss of CHH or CG methylation at rDNA loci. We show that NOR2 genes are relatively hypermethylated than NOR4 genes, consistent with findings from other recent studies (Fultz et al., 2023, Mo et al., 2023).

Using NOR sequences of *Arabidopsis* (Fultz et al., 2023) and tomato (Shirasawa and Ariizumi, 2024), we show that in the 45S rRNA gene sequences, occurrence of cytosines is the highest in the CHH context, followed by CG, and the lowest in the CHG context, providing a putative mechanistic basis for higher *NOR2* derepression observed in *cmt2, ddm1, and met1* mutants that display significantly higher losses of CHH or CG methylation than the other mutants. In contrast to the exclusive involvement of CG methylation in mammalian rRNA gene regulation, our study demonstrates a critical role for CMT2-mediated CHH methylation, in addition to the previously established role for CG methylation, in plant rRNA gene regulation

Results

Selective *NOR2* rRNA gene silencing is disrupted in DNA methylation mutants

The rRNA genes in *A. thaliana* are organized into two tandem arrays on NORs, one each on chromosomes 2 (*NOR2*), and 4 (*NOR4*) (Figure 1). In the reference strain Col-0, *NOR2* is 5.5 Mb and *NOR4* is 3.9 Mb, with ~550 and ~390 tandem repeats of 45S rRNA genes,

144 respectively (Fultz et al., 2023) (Figure 1). The 18S, 5.8S, and 25S rRNA sequences are
145 identical among 45S rRNA genes, but variation exists in the internal transcribed spacer (ITS)
146 and the external transcribed spacer (ETS) regions. Four distinct variants, named VAR1
147 through VAR4, had previously been defined based on the length polymorphism in the 3' ETS
148 region (Pontvianne et al., 2010) (Figure 1B-C). A recent study in the Col-0 ecotype identified
149 74 rRNA gene subtypes, based on length and sequence variation (Fultz et al., 2023).
150 Nonetheless, the primers that amplify the four rRNA subtypes bind to most of the repeats
151 from both NORs. Of these, VAR1, VAR2, and a subset of VAR3 (VAR3a) lack HindIII sites in
152 the 3' ETS region, but the remaining variants (VAR3b,c and VAR4) have a HindIII site
153 (Chandrasekhara et al., 2016, Mohannath et al., 2016) (Figure 1C). During development, the
154 rRNA gene variants that map primarily to *NOR2* (VAR1, VAR3a) are selectively silenced as
155 a consequence of dosage control. In contrast, the variants that map primarily to *NOR4*
156 (VAR2, VAR3c, and VAR4) remain active (Figure 1D)(Chandrasekhara et al., 2016).
157 To determine the relative impact of loss of CG, CHG, and CHH methylation on
158 selective *NOR2* rRNA gene silencing, we analysed rRNA variant expression in mutants
159 defective for DNA methylation, including *ddm1*, *cmt2*, *met1*, *cmt3*, and *drm2* mutants. In
160 these mutants and the WT-Col-0 strain, we performed RT-PCR analysis using RNA isolated
161 from 4-week-old leaf tissues. VAR1 type rRNA genes constitute ~50% of total 45S rRNA
162 genes, and most of them map to *NOR2* and undergo selective silencing during development
163 (Chandrasekhara et al., 2016, Pontvianne et al., 2010). Our results showed that among the
164 DNA methylation mutants, VAR1 expression levels were found to be higher in *cmt2, ddm1,*
165 and *met1* mutants than the other mutants (Figure 2, Figure S1). In contrast, the *cmt3* and
166 *drm2* mutants have displayed modest levels of VAR1 expression (Figure 2, Figure S1).
167
168 **_NOR2_ rRNA genes are hypermethylated while _NOR4_ rRNA genes are hypomethylated**
169 **in Col-0**
170 We performed methylation analysis of rRNA variants using HpaII-digested genomic DNA
171 (gDNA) from Col-0 and *met1* mutants (Figure 3). Because the rRNA variant-defining 3' ETS
172 region lacks HpaII sites, HpaII digestion of gDNA does not impact PCR amplification of this
173 region. Therefore, we chose to separate HpaII-digested and HpaII-undigested fractions of
174 gDNA by resolving them on an agarose gel. The fragments that remained at the top of the
175 gel (>20 kb) constituted the HpaII-undigested fractions, while those resolved at the 0.6-1.0
176 kb range constituted the HpaII-digested fractions (Figure 3A, left panel). Both the digested
177 and the undigested fractions were gel-eluted, followed by PCR amplification of rRNA
178 variants. Through this analysis, we identified the rRNA variants that were enriched in either
179 HpaII-digested or undigested fractions. The PCR data revealed VAR2 genes from *NOR4* to

180 be the most predominant in Col-0 among the HpaII-digested products, indicating relative
181 hypomethylation of *NOR4* genes compared to *NOR2*-localized VAR1 genes (Figure 3A,
182 lanes 1 and 2, right panel). However, in *met1* mutants, used as a control, all rRNA variants
183 were amplified proportionate to their composition due to loss of cytosine methylation in all of
184 them (Figure 3A, lanes 3 and 4, right panel,).
185 In another experiment, we subjected gDNA to digestion by McrBC, an enzyme that
186 preferentially digests DNA if its recognition site ($R^mC(N_{40\text{-}3000})R^mC$) consists of methylated
187 cytosines. McrBC digestion of gDNA followed by PCR amplification of rRNA variants
188 revealed that VAR1 was digested the most and VAR2 the least (Figure 3B), indicating that
189 *NOR2* genes are hypermethylated in contrast to *NOR4* genes, consistent with recent
190 findings in *Arabidopsis* which employed sequencing-based methylation analysis of rRNA
191 variants (Fultz et al., 2023, Mo et al., 2023).
192
193 **_NOR2_ rRNA genes are hypermethylated, while _NOR4_ rRNA genes are hypomethylated**
194 **in the introgression line $Col^{Sf\text{-}NOR4}$**
195 In a previous study, we demonstrated that an introgression line named $Col^{Sf\text{-}NOR4}$ comprises
196 *NOR2* from Col-0 (containing VAR1 and VAR3 genes) and *NOR4* from the Sf-2 ecotype
197 (Chandrasekhara et al., 2016) (Figure 4A). Sf-2 has only VAR1 type of rRNA genes, but they
198 can be differentiated from VAR1 genes of Col-0 by HindIII digestion. Sf-2 VAR1 genes have
199 a HindIII site in their 3' ETS region, while Col-0 VAR1 genes lack it (Chandrasekhara et al.,
200 2016). In $Col^{Sf\text{-}NOR4}$, Sf-2 *NOR4* genes are active, though they are similar in sequence to the
201 silenced Col-0 *NOR2* (VAR1) genes (Chandrasekhara et al., 2016). However, Col-0 *NOR2*
202 genes are still selectively silenced in $Col^{Sf\text{-}NOR4}$ (Chandrasekhara et al., 2016). Therefore, we
203 analyzed this introgression line to determine if VAR1 type of genes residing in *NOR2* and
204 *NOR4* of $Col^{Sf\text{-}NOR4}$ are differentially methylated or not, using similar methylation assays as
205 described above. In one experiment, gDNA of $Col^{Sf\text{-}NOR4}$ was subjected to HpaII digestion,
206 followed by gel elutions of the undigested and the digested fractions. The gel-eluted DNA
207 samples were then subjected to PCR amplification of rRNA variants followed by HindIII
208 digestion. In control samples (no HpaII), HindIII digestion of PCR-amplified rRNA variants
209 resulted in the expected products, which include digested Sf2-VAR1 genes, undigested Col-
210 0 VAR1 genes, and partially digested Col-0 VAR3 genes (Figure 4B, lanes 1 and 2, top right
211 gel image, and Figure 4C) (Chandrasekhara et al., 2016). However, HindIII digestion of the
212 PCR products obtained from the gel-purified HpaII-digested fraction as the template
213 revealed that Col-0 VAR1 genes predominantly constitute the HpaII-undigested fraction
214 (Figure 4B, lanes 3 and 4, top right gel image, and Figure 4C). On the other hand, we
215 observed a significant increase in the Sf-2 VAR1 genes in the HpaII-digested fraction (Figure

216 4B, lanes 3 and 4, bottom right gel image, and Figure 4C) compared to the undigested
217 fraction (Figure 4B, lanes 3 and 4, top right gel image, and Figure 4C). These data indicate
218 hypermethylation of Col-0 *NOR2* genes and hypomethylation of Sf-2 *NOR4* genes, despite
219 the presence of the VAR1 type of genes on both the NORs in the $Col^{Sf\text{-}NOR4}$ introgression line.
220 In another experiment, gDNA of $Col^{Sf\text{-}NOR4}$ was first digested with McrBC, followed by
221 PCR amplification of rRNA variants. We then digested these PCR products with HindIII and
222 resolved them using regular gel electrophoresis. HindIII-digested control PCR products (no
223 McrBC digestion) behaved as expected based on the presence or the absence of HindIII
224 sites (Figure 4D-E, lanes 1 and 2). However, the McrBC digestion patterns of the rRNA
225 variants (Figure 4D-E) were the opposite of the experimental results involving HpaII
226 digestion (compare to Figure 4B-C). Predominantly, the Sf-2 VAR1 genes constituted the
227 McrBC-undigested fraction, while the Col-0 VAR1 genes constituted the McrBC-digested
228 fraction (Figure 4D-E, lanes 3 and 4). We also observed complete digestion of the Col-0
229 VAR3 (from *NOR2*) genes by McrBC (Figure 4D, lane 3). These data again demonstrate that
230 *NOR4* genes are hypomethylated and *NOR2* genes are hypermethylated in $Col^{Sf\text{-}NOR4}$.
231 In Figures 3 and 4, resistance to HpaII digestion indicates the presence of CG and
232 CHG methylation, while digestion by McrBC indicates the prevalence of CG, CHG, and CHH
233 methylation. Based on these data, we conclude that *NOR2* genes are hypermethylated
234 compared to *NOR4* genes in all cytosine contexts, and this status do not change irrespective
235 of the type of rRNA variants present on *NOR2* or *NOR4*.
236
237 **The rRNA gene methylation heat maps reveal a critical role for CMT2-mediated CHH**
238 **methylation in rRNA gene silencing**
239 Using published whole-genome bisulfite sequencing data (Stroud et al., 2013), we generated
240 heatmaps of cytosine methylation for a 45S rRNA reference gene sequence (Data File S1)
241 using Methylpy (Schultz et al., 2015). DDM1 is required for cytosine methylation in all
242 sequence contexts predominantly in heterochromatin than euchromatin (Jeddeloh et al.,
243 1999, Lippman et al., 2004, Vongs et al., 1993, Zemach et al., 2013). *NOR2* primarily exists
244 as heterochromatin while *NOR4* exists as euchromatin (Figure 3)(Fultz et al., 2023, Mo et al.,
245 2023), which correlates with their differential rRNA gene expression (active *NOR4* vs
246 inactive *NOR2*)(Fultz et al., 2023, Mohannath et al., 2016, Chandrasekhara et al., 2016).
247 Therefore, we presume that the loss of cytosine methylation shown in methylation heat maps
248 for all the mutants (Figure 5) largely reflects losses from *NOR2* than *NOR4*.
249 The rDNA cytosine methylation heatmaps show that the entire rRNA gene
250 sequences are methylated in all sequence contexts (Figure 5, see Col-0 column in CG, CHG,
251 and CHH tracks), consistent with recent findings (Fultz et al., 2023). Among the mutants, the

highest overall loss of CHH methylation was observed in *cmt2*, followed by *ddm1* and *met1* mutants (Figure 5). Indeed, these mutants also show higher *NOR2* gene silencing disruption than the other mutants (Figure 2, Figure S1). Interestingly, in *drm1drm2* mutants, although the overall CHH methylation loss is significantly lesser than that of *cmt2* mutants, the losses are comparable around the gene promoter (GP) and the upstream region or are even slightly higher in *drm2* mutants (Figure 5). These results indicate two things; one, RdDM-independent CMT2, primarily methylates CHH sites throughout the gene sequences, while RdDM-dependent DRM primarily methylates CHH sites present in the GP and its upstream sequences. Second, despite the losses of CHH methylation around the promoter region being comparable between *cmt2* and *drm2* mutants (Figure 5), the disruption of rRNA gene silencing is significantly more in *cmt2* than in *drm2* mutants (Figure 2), suggesting a role for gene body CHH methylation in rRNA gene silencing. Recent studies, including one on DDM1, demonstrate that gene body methylation also play a role in gene silencing (Lee et al., 2023a, Shahzad et al., 2025, Williams et al., 2023). Further, the CG methylation levels in *cmt2* mutants are comparable to those of WT-Col-0 (Figure 5), yet the loss of *NOR2* gene silencing is among the highest in *cmt2* mutants (Figure 2, Figure S1), indicating that CHH methylation loss is sufficient for releasing rRNA gene silencing. As a corollary, the presence of CG methylation is not sufficient for rRNA gene silencing.

The *met1* and *ddm1* mutants showed near complete loss of CG methylation at rDNA loci, while other mutants hardly lost any CG methylation (Figure 5). Also, the *met1* mutants showed some loss of CHH and CHG methylation at few sites within rRNA gene body sequences but gained some CHH methylation in the gene promoter region, not in the gene body (Figure 5). Given these data, we attribute the significant disruption of *NOR2* gene silencing observed in *met1* mutants (Figure 2) to the near-complete loss of CG methylation in them (Figure 5), without ruling out a minor contribution from the CHH methylation loss observed in a small portion the gene body. CHH hypermethylation around the promoter region has also been observed In *hda6* mutants which display a loss of CG and CHG methylation and disruption of *NOR2* gene silencing (Chandrasekhara et al., 2016, Earley et al., 2010, Mohannath et al., 2016). Consistent with our conclusion that both CG and CHH methylation are required for rRNA gene silencing, we hypothesize that the disruption of *NOR2* gene silencing observed in *hda6* mutants is at least partly due to their CG methylation loss (Earley et al., 2010). Moreover, another study indicates that HDA6 could affect gene silencing without significantly altering DNA methylation (Hristova et al., 2015).

Next, given the modest release of *NOR2* rRNA gene silencing in *cmt3* mutants despite near complete loss of CHG methylation in them (Figures 2 and 5), we conclude that the CHG methylation has a minimal role in rRNA gene silencing. Based on the results

288 discussed so far, we propose that combination of MET1-mediated CG and CMT-mediated,
289 RdDM-independent CHH methylation is required for selective rRNA gene silencing.
290 Comparable losses of *NOR2* gene silencing disruption in *ddm1* mutants, which display near
291 complete loss of cytosine methylation in all sequence contexts, and *cmt2* mutants, which
292 display a loss of most of CHH methylation (Figures 2 and 5), indicate that MET1-mediated
293 CG and CMT2-mediated CHH methylation act in a complementary manner, rather than
294 synergistically, in rRNA gene silencing.

295 Another observation of some interest is that lower levels of CHG and CHH
296 methylation losses at rDNA loci in *met1* mutants are not uniform, rather they occur at the
297 same two sites for the CHG and CHH methylation losses (Figure 5). One site encompasses
298 the 5'ETS region, while the other starts near the end of 18S and ends near the middle of 25S
299 (Figure 5, compare CHG and CHH tracks of *met1* mutants). Interestingly, in the latter region,
300 *cmt2* mutants also show some loss of CG methylation (Figure 5, compare CHH track of *met1*
301 mutants and CG track of *cmt2* mutants). These results suggest as if some specific sites in
302 rRNA gene body require both CMT2 and MET1 for efficient CG and CHH methylation, but
303 we are not aware of any such existing links between these two methyltransferases.

304 The data depicted in the methylation heat maps (Figure 5) depicting varying losses of
305 CG, CHG, and CHH methylation at rDNA loci and disruption of *NOR2* gene silencing in *met1*,
306 *cmt3*, and *drm2* mutants are consistent with findings from previous studies (Cokus et al.,
307 2008, Pontvianne et al., 2013). But notably, *ddm1* and *cmt2* mutants were not included in
308 these studies. Studying these mutants proved crucial in establishing a critical role for CMT2-
309 mediated CHH methylation, in combination with CG methylation, in rRNA gene silencing.
310

311 **Cytosine occurrence in rRNA genes is the highest in the CHH context followed by CG**
312 **and the lowest in the CHG context**

313 We wondered why CHH methylation loss significantly impacts *NOR2* rRNA gene silencing,
314 despite the *NOR2* genes showing relatively lower levels of CHH methylation (Fultz et al.,
315 2023, Mo et al., 2023). To address this question, we analyzed the distribution of cytosines in
316 CG, CHG, and CHH sequence contexts across all the 45S rRNA gene sequences, obtained
317 from a recent study (Fultz et al., 2023). From these sequences, we depict 2 reference
318 sequences, which commonly represent *NOR2* and/or *NOR4* (Figure 4A and Data File S2).
319 We analyzed the gene sequences in five categories: gene promoter (GP), spacer promoter
320 (SP), GP upstream sequence, Sal clusters and other sequences of intergenic space (IGS),
321 and the gene body, which includes the entire transcribed (pre-45S rRNA) sequence. In *A.*
322 *thaliana*, the -55 to +6 region with respect to the transcription start site (+1) in the 45S rRNA
323 genes constitutes the minimal rRNA gene promoter (hereafter referred to as the gene

324 promoter) (Doelling et al., 1993, Doelling and Pikaard, 1995), which occurs only once per
325 gene repeat (Figure 4A). The GP is 100% conserved in 96% of the gene repeats, while the
326 remainder of the repeats carries one to a few mismatches (Fultz et al., 2023). The GP has
327 eight cytosines, but strikingly, none of them exist in the CG context. Six (75%) exist in the
328 CHH context, and the remaining two (25%) exist in the CHG context (Figure 4A).

329 Similarly, we analysed the predicted GP regions in the recently assembled tomato
330 *NOR2*, constituting ~1500 45S rRNA genes (Shirasawa and Ariizumi, 2024), and the
331 previously published tomato 45S rRNA gene promoter sequence (Doelling and Pikaard,
332 1995). 98% of the gene repeats show 100% homology to the predicted GP sequence (-55 to
333 +6) and the remaining repeats showed one to few mismatches (Shirasawa and Ariizumi,
334 2024). This predicted GP has 12 cytosines, of which 10 (~83%) exist in the CHH context, 2
335 (~17%) in the CHG context, and none in the CG context (Figures 4B-C and S2, Data File S3)
336 (Doelling and Pikaard, 1995, Shirasawa and Ariizumi, 2023, Shirasawa and Ariizumi, 2024).
337 Similar cytosine distributions were found in the predicted GPs of other plant species (Figure
338 4B-C) (Doelling and Pikaard, 1995). Further, we analyzed ~270 bp immediate upstream
339 region of the GP, in which, out of 45-46 cytosines, 4 each (9% each) exist in CG and CHG
340 contexts, while 35-36 (81-82%) exist in the CHH context (Figure 4A). Likewise, in the
341 immediate upstream region of the predicted GP in tomato 45S rRNA gene sequence up to
342 413 bp, cytosine distribution is largely skewed towards CHH sites. Out of 43 cytosines, we
343 found 10 (23%) in CG, 3 (7%) in CHG, and 30 (70%) in CHH context (Figure S2).

344 Next, we tabulated cytosine distribution in the Arabidopsis spacer promoters (SPs),
345 whose number varies from 0 to 4, with 1 SP being the most common in both *NOR2* and
346 *NOR4* (Figure 4A) (Fultz et al., 2023). The SPs share homology with the GP sequence and
347 can program low-level transcription by RNA polymerase I (Doelling et al., 1993). Each SP
348 has a total of 14 cytosines, of which 11 (~79%) are in the CHH context, 2 (~14%) are in the
349 CHG context, and 1 (~7%) in the CG context (Figure 4A, Data File S2). Further, we
350 calculated cytosine distribution in other regions of IGS, including the Sal clusters, which are
351 made of 20-21 bp repeats containing a SalI restriction site, and other interspersed
352 sequences (Fultz et al., 2023). Interestingly, in this region, we found predominant occurrence
353 of CG (52-53 %) over CHG (25-26 %) and CHG (21-22 %) sites, even among IGS regions
354 varying in length from ~350 to 465 (Figures 4A, Data File S2). If we consider the total
355 cytosines across the entire 45S rRNA gene sequence, the frequency of CHH sites (45-46%)
356 ranks first while the frequencies of CG (35%) and CHG sites (19-20%) rank second and third,
357 respectively (Figure 4A).

358 Similar analysis of tomato IGS sequences did not yield any IGS elements containing
359 Sal repeats or sequence elements which shared homology with the predicted GP. In the

360 predicted IGS of tomato, although we found that the number of CHH sites(139/256) is still
361 the highest among three contexts, the number of CG sites (99/256) increase substantially in
362 this region (Figure S2). The number of CHG sites (18) is the lowest (Figure S2). Overall
363 cytosine distribution pattern in tomato 45S rRNA gene sequences mirror that of Arabidopsis,
364 with number of CHG sites > CG sites > CHG sites (Figure S2).

365 Recent studies have shown that the gene body methylation also plays a role in gene
366 regulation (Lee et al., 2023a, Shahzad et al., 2025, Williams et al., 2023), and in Arabidopsis,
367 the entire rRNA gene sequences are heavily methylated (Figure 2) (Fultz et al., 2023).
368 Therefore, we extended cytosine distribution analysis to rRNA gene bodies, wherein we
369 found the occurrence of more CHH sites than CG and CHG, both in *Arabidopsis* (49%
370 CHH > 32% CG > 19% CHG) and tomato (46% CHH > 35% CG > 18% CHG) (Figures 4A
371 and S2, Data Files S2-S3). Similar trends were observed when we considered the entire 45S
372 rRNA gene sequences (*Arabidopsis*: 46% CHH > 35% CG > 20% CHG, tomato: 48% CHH >
373 35% CG > 17% CHG) (Figures 4A and S2, Data Files S2-S3). Collectively, these findings
374 provide a putative mechanistic basis for the maximum disruption of *NOR2* rRNA gene
375 silencing in mutants that displayed higher loss of CHH (*cmt2, ddm1, and met1*) or CG
376 methylation (*met1* and *ddm1*) than the other mutants. Importantly, these results define a
377 novel critical role for CHH methylation in regulating 45S rRNA genes in plants.

378 In contrast, when we analyzed human rDNA promoter sequences (Zhou et al., 2016),
379 we found that, out of 65 cytosines, 26 are in CG (~40%; the highest among the three), 19 in
380 CHG (~29%), and 20 in CHH (~31%) contexts (Figure S3, columns 2-3, Data File S4). Even
381 when we included an extended upstream sequence as part of the rDNA promoter, according
382 to another study (Uemura et al., 2012), the cytosine distribution trend remained the same
383 (Figure S3, columns 4-5, Data File S4). Similarly, we found the predominant occurrence of
384 CG sites in the gene bodies (Figure S3, the last two columns, Data File S4). These results
385 are consistent with the mammalian rRNA gene regulation, which is almost entirely dictated
386 by CG methylation (Bernstein et al., 2007, Priyadarshini et al., 2023, Zhou et al., 2016).
387 These findings also correlate with the evolutionary loss of chromomethylases (CMTs) in
388 mammals. CMTs are plant-specific, which primarily methylate CHG and CHH sites (Bewick
389 et al., 2017). Collectively, these findings indicate the presence of evolutionarily divergent
390 mechanisms of rRNA gene silencing in plants and mammals.

391

392

393 **Discussion**

394 The study primarily provides two new insights. First, RdDM-independent CMT2, mediates
395 majority of the CHH methylation at rDNA loci (Figure 5). Second, the loss of CMT2-mediated

396 CHH methylation is sufficient for disrupting selective *NOR2* gene silencing (Figures 2 and 5).
397 A recent study in a different plant species highlights a role of non-CG methylation in plant
398 rRNA gene silencing (Matyášek et al., 2024), but it did not include CMT2. Our data also
399 capture findings from a previous study in underscoring a critical role played by CG
400 methylation in rRNA gene silencing (Figures 2, 3 and 5). Based on our collective findings, we
401 propose a model stating that a combination of CG methylation and CMT-mediated RdDM-
402 independent CHH methylation is required for rRNA gene silencing (Figure 7). Losing any
403 one of them is sufficient for releasing the rRNA gene silencing. In *ddm1* mutants, CG and
404 CHH methylation are nearly wiped out, their NOR2-residing VAR1 expression levels are
405 comparable to that of *cmt2* mutants, in which only CHH methylation is nearly wiped out
406 (Figures 2 and 5). These data prompted us to further proposed that MET1-mediated CG and
407 CMT2-mediated CHH methylation act complementarily, rather than additively, in silencing
408 rRNA genes.
409 Based on the most abundant CG methylation found at NOR loci (Cokus et al., 2008,
410 Fultz et al., 2023, Mérai et al., 2014, Pontvianne et al., 2013), it is fairly understandable
411 mechanistically how CG methylation could play a role in rRNA gene silencing. However,
412 relative methylation levels of CHH being the lowest at rDNA loci, it has not been obvious
413 how CHH methylation loss would disrupt rRNA gene silencing. To address this gap, we
414 asked an important question-cytosine methylation of which regions play a role in rRNA gene
415 silencing? To address this question, we analyzed cytosine distribution among the three
416 sequence contexts (CG, CHG, and CHH) in regulatory and gene bodies of the rRNA genes.
417 In the characterized regulatory elements constituting GP and SP, CHH site occurrence
418 (17/22) is overwhelmingly high compared to either CG (1/22) or CHG (4/22) and the trend
419 remained the same even when we analyzed ~270 bp upstream of GP region or the gene
420 body (Figure 6A). Likewise, analysis of comparable regions from tomato rRNA sequences
421 also yielded the similar cytosine distribution heavily in favour of CHH over CG or CHG sites
422 (Figure S2). These findings provide a potential mechanistic basis to explain how CHH
423 methylation could play a critical role in rRNA gene silencing. When the number of CHH sites
424 are overwhelmingly high in a region of regulatory importance, low levels of CHH methylation
425 can be compensated by higher number of CHH sites. For instance, in the GP and SP
426 regions combined, CHH site frequency is 17- and 4.3-fold higher than CG and CHG sites,
427 respectively (Figure 6A). However, Sal-repeats-containing IGS (minus SP) region, is highly
428 CG-rich (CG- 189 sites, CHG- 91 sites, and CHH- 75 sites, when we considered the most
429 commonly occurring 2-Sal cluster scenario) (Figure 6A), which explains why CG methylation
430 loss significantly disrupts rRNA gene silencing (Figures 2, 5 and 6). In the predicted
431 comparable sequences of tomato NORs, we could not find Sal repeats and in this region,

432 CHH occurrence still turned out to be the highest (CG- 109 sites, CHG- 21 sites, and CHH-
433 167 sites) (Figure S2), suggesting predominant occurrence of CG and CHH sites in the IGS
434 and promoter regions, although in varying proportions.

435 CMT2 and CMT3 methylate DNA through the dual binding of H3K9 di-
436 methylation (H3K9me2)-containing nucleosomes via their bromo adjacent homology (BAH)
437 and Chromo domains (Du et al., 2012). Of note, H3K9 methyltransferases are required for
438 rRNA variant-specific silencing in *A. thaliana* (Pontvianne et al., 2012). However, the loss of
439 CHH methylation at rDNA loci has more impact on *NOR2* derepression than the loss of CHG
440 methylation, presumably due to higher occurrence of cytosines in the CHH context than the
441 CHG context in the rRNA genes (both in the regulatory elements and gene body) (Figures 2,
442 5, and 6).

443 DDM1 mediates CHH methylation by CMT2 (Zemach et al., 2013) and therefore it is
444 reasonable to find levels of CHH methylation loss and *NOR2* gene silencing in *ddm1*
445 mutants comparable to that of *cmt2* mutants (Figures 2-3). Recent findings have shown that
446 DDM1 deposits histone variant H2A.W, which marks plant heterochromatin, onto potentially
447 mobile transposable elements (TEs), resulting in their transcriptional gene silencing
448 (Osakabe et al., 2021). We speculate that a similar mechanism, involving DDM1-mediated
449 histone H2A.W deposition, is also involved in *NOR2* rRNA gene silencing.

450 Our data also indicate a role for gene body methylation in rRNA gene silencing. For
451 example, in *cmt2* and *drm2* mutants, CG methylation is largely intact, little to no change in
452 CHG methylation and comparable loss of CHH methylation in the promoter and the
453 upstream sequences but gene body CHH methylation loss and NOR2 gene silencing
454 disruption are significantly higher in *cmt2* than *drm2* mutants (Figures 2 and 5). These data
455 suggest a role for gene body CHH methylation in rRNA gene silencing. Similar role for gene
456 body CG methylation is highly likely, given its role in the regulation of various genomic loci
457 (Lee et al., 2023a, Shahzad et al., 2025, Williams et al., 2023).

458 In contrast, rRNA gene silencing is entirely mediated by CG methylation in mammals.
459 For example, human rDNA promoters are mostly methylated in the CG context and their
460 dysregulation has been linked to several types of cancers (Priyadarshini et al., 2023,
461 Bacalini et al., 2014, Ghoshal et al., 2004, Karahan et al., 2015, Raval et al., 2012, Zhou et
462 al., 2016). Moreover, cytosines occur predominantly in the CG context in the human rRNA
463 gene promoters and gene bodies (Figure S3). CHG and CHH methylation are largely absent
464 in mammals, which correlates with their evolutionary loss of CMTs that primarily methylate
465 CHG and CHH (Bernstein et al., 2007, Bewick et al., 2017, Henderson and Jacobsen, 2007).
466 Notably, spacer promoters in animal models (e.g., frog species *Xenopus laevis*) significantly
467 contribute to the enhancement of rRNA gene transcription (De Winter and Moss, 1986). In

468 contrast, spacer promoters have minimal contribution to rRNA gene transcription in plant
469 species (e.g. *Arabidopsis thaliana*) (Doelling et al., 1993). These findings indicate the
470 evolution of divergent rRNA gene regulatory pathways in plants and animals.
471 The silent *NOR2* genes are hypermethylated in all cytosine contexts (CG, CHG, and
472 CHH) and exist in chromatin with decreased accessibility state than the active *NOR4* rRNA
473 genes, irrespective of the type of rRNA variants on them (Figures 3-4) (Fultz et al., 2023, Mo
474 et al., 2023). Despite the striking similarities in rRNA gene sequences between *NOR2* and
475 *NOR4*, why rRNA genes on *NOR2* are selectively hypermethylated and silenced? It has
476 been speculated that silencing from a stretch of NOR2-flanking transposable elements and
477 transposon remnants that stretch for ~60 kb before the first protein-coding genes are
478 encountered, could potentially spread to *NOR2* (Chandrasekhara et al., 2016). This ~60 kb
479 region is heavily cytosine methylated and carries histone post-translational modifications,
480 which are indicative of transcriptionally repressed heterochromatin. In contrast, NOR4 is
481 flanked by a few transposon-related sequences, with the occurrence of active protein-coding
482 genes within ~3 kb of the NOR4 boundary. However, the question remains to be answered.
483
484 **Materials and Methods**
485 ***Plant material and growth***
486 *A. thaliana* ecotype Col-0 (stock no. CS22681), and mutants *met1-7* (stock no.
487 SALK_076522), *cmt2-3* (stock no. SALK_012874C), and *cmt3-11t* (stock no. SALK_148381),
488 were obtained from the *Arabidopsis* Biological Resource Center (ABRC; http://abrc.osu.edu).
489 *drm2-2b* (stock no. SAIL_70_E12) and $Col^{Sf\text{-}NOR4}$ (Chandrasekhara et al., 2016, Lee and
490 Amasino, 1995) were provided by Andrzej Wierzbicki and Scott Michaels, respectively, and
491 *ddm1-2* was provided by Eric Richards. Plants were grown in soil in a plant growth room
492 under a 16-h light/8-h dark photoperiod cycle with 50–55% humidity and temperature of 23–
493 25°C.
494
495 ***RNA isolation***
496 Four-week-old leaf tissue of individual plants was frozen in liquid nitrogen and ground into a
497 fine powder. RNeasy Plant Mini Kit (Qiagen) was used to extract total RNA from ground
498 powder. Total RNA was then treated with Turbo DNA-free kit (Invitrogen) to eliminate
499 contaminating DNA.
500
501 ***PCR and RT-PCR assays***
502 For PCR of genomic DNA to amplify all rRNA variants, PCR amplification was conducted
503 using 22-30 cycles (depending on the source of DNA) of 30 sec at 95°C, 30 sec at 55°C–

504 60°C, and 60 sec at 72°C. For RT–PCR, the reverse transcription reaction was performed
505 using 1 µg of total RNA using SuperScript III reverse transcriptase (Invitrogen). One
506 microliter (~100 ng) of reverse transcription product was then used for PCR amplification of
507 rRNA variable regions or actin gene control using 30 cycles of 30 sec at 94°C, 30 sec at
508 55°C, and 60 sec at 72°C. In all the PCR or RT-PCR reactions, primers 5'allvar and 3'allvar
509 were used to amplify rRNA variable regions (all four variant types). PCR and RT–PCR
510 products were resolved by electrophoresis on 2%–2.5% agarose gels in TBE buffer.
511 Sequences of primers used in this study are given in Figure S10. Pixel intensities for bands
512 in Figures 1, S2, 4B, and 5B were calculated using Quantity one software (Bio-Rad).
513
514 ***Generation of DNA methylation heat maps and rRNA gene cytosine methylation***
515 ***frequencies***
516 Whole genome bisulfite sequencing data (GSE39901) published by Stroud et al.
517 (2013)(Stroud et al., 2013), was used to assess the methylation state of rDNA in various
518 methylation mutants. The sequencing data were analysed using Methylpy (Schultz et al.,
519 2015). The reads were mapped to a converted 45S rDNA reference sequence, allowing a
520 single mismatch. The methylation state of all cytosines in CG, CHG, and CHH contexts was
521 then analyzed and represented as a fraction of methylated cytosines over the total cytosines
522 in each context. Replicates for a given genotype were merged into a single file.
523
524 ***DNA isolation from leaf tissue and agarose gel pieces (gel elution).***
525 Genomic DNA (gDNA) was isolated from the leaf tissue of 4-week-old plants by using Illustra
526 Nucleon Phytopure extraction kit reagents (GE Healthcare). This gDNA was used for HindIII
527 CAPS assay (Figure S1C), PCR of rRNA variants (Figure 1, topmost panel), methylation
528 analysis of gDNA (Figure 4A left panel, Figure 4B, and Figure 5B, left panel). In some cases,
529 following gDNA PCR or digestion by methylation-sensitive enzymes, the products were
530 resolved on an agarose gel and the DNA fragments were gel-purified using QIAquick gel
531 extraction kit (Qiagen). This gel-purified DNA was subsequently used as a template for
532 downstream PCR amplification of rRNA variants (Figure 4B right panel, Figure S8C) or
533 HindIII CAPS assay (Figure 5B right panel). DNA from the EZ-Tn5 transposase-treated
534 nuclei was isolated using the cetyl trimethyl ammonium bromide (CTAB) method.
535 The sequences of primers and oligos used in this study are listed in Figure S4.
536
537 **Acknowledgements**
538 This work is supported by: Birla Institute of Science and Technology (BITS) Pilani,
539 Hyderabad campus through a research grant to G.M. (BITS/GAU/ACRG/2019/H0576) and

an Institute Fellowship to G.P.S. Science and Engineering Research Board (SERB), Government of India through Ramanujan Fellowship (SB-S2-RJN-062-2017) and CRG (CRG/2020/002855) research grants to GM, and internship to N.V.P. Department of Biotechnology through research grant (BT/PR38410/GET/119/310/2020) to GM and through it, Junior Research Fellowship to R.T. We profusely thank members of the Pikaard lab for their critique of the manuscript.

Competing interests

The authors declare no competing interests.

Author contributions

N.V.P, R.T., and G.M. planned and designed the research; N.V.P., R.T., G.P.S., and G.M. performed the research; N.V.P, R.T., G.P.S., and G.M. analysed the data; N.V.P, R.T., and G.M. wrote the paper.

Data availability

For this article we analyzed the publicly available/published data, and the details are as follows: The whole genome bisulfite sequencing data of *Arabidopsis thaliana* (WT and mutants) were published by Stroud et al. (2013) (GEO accession# GSM980986). The fully assembled NOR sequences of *Arabidopsis thaliana* (strain Col-0) were published by Fultz et al. (2023) and the sequences are available at GenBank as accessions OR453402 (https://ncbi.nlm.nih.gov/nuccore/OR453402) for *NOR2* and OR453401 (https://ncbi.nlm.nih.gov/nuccore/OR453401) for *NOR4*. Assembled whole genome sequences of tomato (*Solanum lycopersicum*, cultivar Micro-Tom) have been published on a preprint server (https://doi.org/10.1101/2023.10.26.564283) and the sequences are available at DDBJ (accession numbers AP028935–1 AP028946) and KaTomicsDB (https://www.kazusa.or.jp/ tomato).

References

BACALINI, M. G., PACILLI, A., GIULIANI, C., PENZO, M., TRERÉ, D., PIRAZZINI, C., SALVIOLI, S., FRANCESCHI, C., MONTANARO, L. & GARAGNANI, P. 2014. The nucleolar size is associated to the methylation status of ribosomal DNA in breast carcinomas. *BMC Cancer,* 14**,** 361.

BERNSTEIN, B. E., MEISSNER, A. & LANDER, E. S. 2007. The mammalian epigenome. *Cell,* 128**,** 669-81.

BEWICK, A. J., NIEDERHUTH, C. E., JI, L., ROHR, N. A., GRIFFIN, P. T., LEEBENS-MACK, J. & SCHMITZ, R. J. 2017. The evolution of CHROMOMETHYLASES and gene body DNA methylation in plants. *Genome Biol,* 18**,** 65.

576 BRZESKI, J. & JERZMANOWSKI, A. 2003. Deficient in DNA methylation 1 (DDM1) defines a novel
577 family of chromatin-remodeling factors. *J Biol Chem,* 278**,** 823-8.
578 CHANDRASEKHARA, C., MOHANNATH, G., BLEVINS, T., PONTVIANNE, F. & PIKAARD, C. S. 2016.
579 Chromosome-specific NOR inactivation explains selective rRNA gene silencing and dosage
580 control in Arabidopsis. *Genes Dev,* 30**,** 177-90.
581 CHEN, Z. J. & PIKAARD, C. S. 1997. Epigenetic silencing of RNA polymerase I transcription: a role for
582 DNA methylation and histone modification in nucleolar dominance. *Genes Dev,* 11**,** 2124-36.
583 COKUS, S. J., FENG, S., ZHANG, X., CHEN, Z., MERRIMAN, B., HAUDENSCHILD, C. D., PRADHAN, S.,
584 NELSON, S. F., PELLEGRINI, M. & JACOBSEN, S. E. 2008. Shotgun bisulphite sequencing of the
585 Arabidopsis genome reveals DNA methylation patterning. *Nature,* 452**,** 215-9.
586 COPENHAVER, G. P., DOELLING, J. H., GENS, S. & PIKAARD, C. S. 1995. Use of RFLPs larger than 100
587 kbp to map the position and internal organization of the nucleolus organizer region on
588 chromosome 2 in Arabidopsis thaliana. *Plant J,* 7**,** 273-86.
589 COPENHAVER, G. P. & PIKAARD, C. S. 1996a. RFLP and physical mapping with an rDNA-specific
590 endonuclease reveals that nucleolus organizer regions of Arabidopsis thaliana adjoin the
591 telomeres on chromosomes 2 and 4. *Plant J,* 9**,** 259-72.
592 COPENHAVER, G. P. & PIKAARD, C. S. 1996b. Two-dimensional RFLP analyses reveal megabase-sized
593 clusters of rRNA gene variants in Arabidopsis thaliana, suggesting local spreading of variants
594 as the mode for gene homogenization during concerted evolution. *Plant J,* 9**,** 273-82.
595 COSTA-NUNES, P., PONTES, O., PREUSS, S. B. & PIKAARD, C. S. 2010. Extra views on RNA-dependent
596 DNA methylation and MBD6-dependent heterochromatin formation in nucleolar dominance.
597 *Nucleus,* 1**,** 254-9.
598 DE WINTER, R. F. & MOSS, T. 1986. Spacer promoters are essential for efficient enhancement of X.
599 laevis ribosomal transcription. *Cell,* 44**,** 313-8.
600 DOELLING, J. H., GAUDINO, R. J. & PIKAARD, C. S. 1993. Functional analysis of Arabidopsis thaliana
601 rRNA gene and spacer promoters in vivo and by transient expression. *Proc Natl Acad Sci U S*
602 *A,* 90**,** 7528-32.
603 DOELLING, J. H. & PIKAARD, C. S. 1995. The minimal ribosomal RNA gene promoter of Arabidopsis
604 thaliana includes a critical element at the transcription initiation site. *Plant J,* 8**,** 683-92.
605 DU, J., ZHONG, X., BERNATAVICHUTE, Y. V., STROUD, H., FENG, S., CARO, E., VASHISHT, A. A.,
606 TERRAGNI, J., CHIN, H. G., TU, A., HETZEL, J., WOHLSCHLEGEL, J. A., PRADHAN, S., PATEL, D. J.
607 & JACOBSEN, S. E. 2012. Dual binding of chromomethylase domains to H3K9me2-containing
608 nucleosomes directs DNA methylation in plants. *Cell,* 151**,** 167-80.
609 EARLEY, K. W., PONTVIANNE, F., WIERZBICKI, A. T., BLEVINS, T., TUCKER, S., COSTA-NUNES, P.,
610 PONTES, O. & PIKAARD, C. S. 2010. Mechanisms of HDA6-mediated rRNA gene silencing:
611 suppression of intergenic Pol II transcription and differential effects on maintenance versus
612 siRNA-directed cytosine methylation. *Genes Dev,* 24**,** 1119-32.
613 FULTZ, D., MCKINLAY, A., ENGANTI, R. & PIKAARD, C. S. 2023. Sequence and epigenetic landscapes of
614 active and silent nucleolus organizer regions in Arabidopsis. *Sci Adv,* 9**,** eadj4509.
615 GERBI, S. A. 1986. The evolution of eukaryotic ribosomal DNA. *Biosystems,* 19**,** 247-58.
616 GHOSHAL, K., MAJUMDER, S., DATTA, J., MOTIWALA, T., BAI, S., SHARMA, S. M., FRANKEL, W. &
617 JACOB, S. T. 2004. Role of human ribosomal RNA (rRNA) promoter methylation and of
618 methyl-CpG-binding protein MBD2 in the suppression of rRNA gene expression. *J Biol Chem,*
619 279**,** 6783-93.
620 GRUMMT, I. 2013. The nucleolus—guardian of cellular homeostasis and genome integrity.
621 *Chromosoma,* 122**,** 487-97.
622 HANNAN, K. M., SANIJ, E., ROTHBLUM, L. I., HANNAN, R. D. & PEARSON, R. B. 2013. Dysregulation of
623 RNA polymerase I transcription during disease. *Biochim Biophys Acta,* 1829**,** 342-60.
624 HENDERSON, I. R. & JACOBSEN, S. E. 2007. Epigenetic inheritance in plants. *Nature,* 447**,** 418-24.

HRISTOVA, E., FAL, K., KLEMME, L., WINDELS, D. & BUCHER, E. 2015. HISTONE DEACETYLASE6 Controls Gene Expression Patterning and DNA Methylation-Independent Euchromatic Silencing. *Plant Physiol,* 168**,** 1298-308.

JEDDELOH, J. A., STOKES, T. L. & RICHARDS, E. J. 1999. Maintenance of genomic methylation requires a SWI2/SNF2-like protein. *Nat Genet,* 22**,** 94-7.

KARAHAN, G., SAYAR, N., GOZUM, G., BOZKURT, B., KONU, O. & YULUG, I. G. 2015. Relative expression of rRNA transcripts and 45S rDNA promoter methylation status are dysregulated in tumors in comparison with matched-normal tissues in breast cancer. *Oncol Rep,* 33**,** 3131-45.

LAW, J. A. & JACOBSEN, S. E. 2010. Establishing, maintaining and modifying DNA methylation patterns in plants and animals. *Nat Rev Genet,* 11**,** 204-20.

LEE, I. & AMASINO, R. M. 1995. Effect of Vernalization, Photoperiod, and Light Quality on the Flowering Phenotype of Arabidopsis Plants Containing the FRIGIDA Gene. *Plant Physiol,* 108**,** 157-162.

LEE, S., CHOI, J., PARK, J., HONG, C. P., CHOI, D., HAN, S., CHOI, K., ROH, T. Y., HWANG, D. & HWANG, I. 2023a. DDM1-mediated gene body DNA methylation is associated with inducible activation of defense-related genes in Arabidopsis. *Genome Biol,* 24**,** 106.

LEE, S. C., ADAMS, D. W., IPSARO, J. J., CAHN, J., LYNN, J., KIM, H. S., BERUBE, B., MAJOR, V., CALARCO, J. P., LEBLANC, C., BHATTACHARJEE, S., RAMU, U., GRIMANELLI, D., JACOB, Y., VOIGT, P., JOSHUA-TOR, L. & MARTIENSSEN, R. A. 2023b. Chromatin remodeling of histone H3 variants by DDM1 underlies epigenetic inheritance of DNA methylation. *Cell,* 186**,** 4100-4116.e15.

LIPPMAN, Z., GENDREL, A. V., BLACK, M., VAUGHN, M. W., DEDHIA, N., MCCOMBIE, W. R., LAVINE, K., MITTAL, V., MAY, B., KASSCHAU, K. D., CARRINGTON, J. C., DOERGE, R. W., COLOT, V. & MARTIENSSEN, R. 2004. Role of transposable elements in heterochromatin and epigenetic control. *Nature,* 430**,** 471-6.

LISTER, R., O'MALLEY, R. C., TONTI-FILIPPINI, J., GREGORY, B. D., BERRY, C. C., MILLAR, A. H. & ECKER, J. R. 2008. Highly integrated single-base resolution maps of the epigenome in Arabidopsis. *Cell,* 133**,** 523-36.

LONG, E. O. & DAWID, I. B. 1980. Repeated genes in eukaryotes. *Annu Rev Biochem,* 49**,** 727-64.

MATYÁŠEK, R., KALFUSOVÁ, R., KUDEROVÁ, A., ŘEHŮŘKOVÁ, K., SOCHOROVÁ, J. & KOVAŘÍK, A. 2024. Transcriptional Silencing of 35S rDNA in Tragopogon porrifolius Correlates with Cytosine Methylation in Sequence-Specific Manner. *Int J Mol Sci,* 25.

MÉRAI, Z., CHUMAK, N., GARCÍA-AGUILAR, M., HSIEH, T. F., NISHIMURA, T., SCHOFT, V. K., BINDICS, J., SLUSARZ, L., ARNOUX, S., OPRAVIL, S., MECHTLER, K., ZILBERMAN, D., FISCHER, R. L. & TAMARU, H. 2014. The AAA-ATPase molecular chaperone Cdc48/p97 disassembles sumoylated centromeres, decondenses heterochromatin, and activates ribosomal RNA genes. *Proc Natl Acad Sci U S A,* 111**,** 16166-71.

MO, W., SHU, Y., LIU, B., LONG, Y., LI, T., CAO, X., DENG, X. & ZHAI, J. 2023. Single-molecule targeted accessibility and methylation sequencing of centromeres, telomeres and rDNAs in Arabidopsis. *Nat Plants,* 9**,** 1439-1450.

MOHANNATH, G., PONTVIANNE, F. & PIKAARD, C. S. 2016. Selective nucleolus organizer inactivation in Arabidopsis is a chromosome position-effect phenomenon. *Proc Natl Acad Sci U S A,* 113**,** 13426-13431.

MOSS, T., LANGLOIS, F., GAGNON-KUGLER, T. & STEFANOVSKY, V. 2007. A housekeeper with power of attorney: the rRNA genes in ribosome biogenesis. *Cell Mol Life Sci,* 64**,** 29-49.

OSAKABE, A., JAMGE, B., AXELSSON, E., MONTGOMERY, S. A., AKIMCHEVA, S., KUEHN, A. L., PISUPATI, R., LORKOVIĆ, Z. J., YELAGANDULA, R., KAKUTANI, T. & BERGER, F. 2021. The chromatin remodeler DDM1 prevents transposon mobility through deposition of histone variant H2A.W. *Nat Cell Biol,* 23**,** 391-400.

PIKAARD, C. S., CHANDRASEKHARA, C., MCKINLAY, A., ENGANTI, R. & FULTZ, D. 2023. Reaching for the off switch in nucleolar dominance. *Plant J,* 115**,** 1185-1192.

PONTVIANNE, F., ABOU-ELLAIL, M., DOUET, J., COMELLA, P., MATIA, I., CHANDRASEKHARA, C., DEBURES, A., BLEVINS, T., COOKE, R., MEDINA, F. J., TOURMENTE, S., PIKAARD, C. S. & SAEZ-VASQUEZ, J. 2010. Nucleolin is required for DNA methylation state and the expression of rRNA gene variants in Arabidopsis thaliana. *PLoS Genet,* 6**,** e1001225.

PONTVIANNE, F., BLEVINS, T., CHANDRASEKHARA, C., FENG, W., STROUD, H., JACOBSEN, S. E., MICHAELS, S. D. & PIKAARD, C. S. 2012. Histone methyltransferases regulating rRNA gene dose and dosage control in Arabidopsis. *Genes Dev,* 26**,** 945-57.

PONTVIANNE, F., BLEVINS, T., CHANDRASEKHARA, C., MOZGOVA, I., HASSEL, C., PONTES, O. M., TUCKER, S., MOKROS, P., MUCHOVA, V., FAJKUS, J. & PIKAARD, C. S. 2013. Subnuclear partitioning of rRNA genes between the nucleolus and nucleoplasm reflects alternative epiallelic states. *Genes Dev,* 27**,** 1545-50.

PREUSS, S. B., COSTA-NUNES, P., TUCKER, S., PONTES, O., LAWRENCE, R. J., MOSHER, R., KASSCHAU, K. D., CARRINGTON, J. C., BAULCOMBE, D. C., VIEGAS, W. & PIKAARD, C. S. 2008. Multimegabase silencing in nucleolar dominance involves siRNA-directed DNA methylation and specific methylcytosine-binding proteins. *Mol Cell,* 32**,** 673-84.

PRIYADARSHINI, N., VENKATARAMA PUPPALA, N., PEROTH JAYAPRAKASH, J., KHANDELIA, P., SHARMA, V. & MOHANNATH, G. 2023. Ribosomal RNA gene downregulation in head and neck squamous carcinoma cells correlates with rDNA promoter hypermethylation. *Gene***,** 147793.

RAVAL, A., SRIDHAR, K. J., PATEL, S., TURNBULL, B. B., GREENBERG, P. L. & MITCHELL, B. S. 2012. Reduced rRNA expression and increased rDNA promoter methylation in CD34+ cells of patients with myelodysplastic syndromes. *Blood,* 120**,** 4812-8.

RHEE, I., BACHMAN, K. E., PARK, B. H., JAIR, K. W., YEN, R. W., SCHUEBEL, K. E., CUI, H., FEINBERG, A. P., LENGAUER, C., KINZLER, K. W., BAYLIN, S. B. & VOGELSTEIN, B. 2002. DNMT1 and DNMT3b cooperate to silence genes in human cancer cells. *Nature,* 416**,** 552-6.

RYMEN, B., FERRAFIAT, L. & BLEVINS, T. 2020. Non-coding RNA polymerases that silence transposable elements and reprogram gene expression in plants. *Transcription,* 11**,** 172-191.

SARADADEVI, G. P., PRIYADARSHINI, N., BERA, A. & MOHANNATH, G. 2020. Together we are on together we are off -a conserved rule for ribosomal RNA (rRNA) gene regulation? *Journal of Plant Biochemistry and Biotechnology,* 29**,** 743-753.

SASAKI, E., KAWAKATSU, T., ECKER, J. R. & NORDBORG, M. 2019. Common alleles of CMT2 and NRPE1 are major determinants of CHH methylation variation in Arabidopsis thaliana. *PLoS Genet,* 15**,** e1008492.

SCHULTZ, M. D., HE, Y., WHITAKER, J. W., HARIHARAN, M., MUKAMEL, E. A., LEUNG, D., RAJAGOPAL, N., NERY, J. R., URICH, M. A., CHEN, H., LIN, S., LIN, Y., JUNG, I., SCHMITT, A. D., SELVARAJ, S., REN, B., SEJNOWSKI, T. J., WANG, W. & ECKER, J. R. 2015. Human body epigenome maps reveal noncanonical DNA methylation variation. *Nature,* 523**,** 212-6.

SHAHZAD, Z., HOLLWEY, E., MOORE, J. D., CHOI, J., CASSIN-ROSS, G., ROUACHED, H., ROBINSON, M. R. & ZILBERMAN, D. 2025. Gene body methylation regulates gene expression and mediates phenotypic diversity in natural Arabidopsis populations. *Nat Plants,* 11**,** 2084-2099.

SHIRASAWA, K. & ARIIZUMI, T. 2023. Near-complete genome assembly of tomato (Solanum lycopersicum) cultivar Micro-Tom. *bioRxiv***,** 2023.10.26.564283.

SHIRASAWA, K. & ARIIZUMI, T. 2024. Near-complete genome assembly of tomato (Solanum lycopersicum) cultivar Micro-Tom. *Plant Biotechnol (Tokyo),* 41**,** 367-374.

STROUD, H., GREENBERG, M. V., FENG, S., BERNATAVICHUTE, Y. V. & JACOBSEN, S. E. 2013. Comprehensive analysis of silencing mutants reveals complex regulation of the Arabidopsis methylome. *Cell,* 152**,** 352-64.

724 TUROWSKI, T. W. & TOLLERVEY, D. 2015. Cotranscriptional events in eukaryotic ribosome synthesis.
725 *Wiley Interdiscip Rev RNA,* 6**,** 129-39.
726 UEMURA, M., ZHENG, Q., KOH, C. M., NELSON, W. G., YEGNASUBRAMANIAN, S. & DE MARZO, A. M.
727 2012. Overexpression of ribosomal RNA in prostate cancer is common but not linked to
728 rDNA promoter hypomethylation. *Oncogene,* 31**,** 1254-63.
729 VIKTOROVSKAYA, O. V. & SCHNEIDER, D. A. 2015. Functional divergence of eukaryotic RNA
730 polymerases: unique properties of RNA polymerase I suit its cellular role. *Gene,* 556**,** 19-26.
731 VONGS, A., KAKUTANI, T., MARTIENSSEN, R. A. & RICHARDS, E. J. 1993. Arabidopsis thaliana DNA
732 methylation mutants. *Science,* 260**,** 1926-8.
733 WILLIAMS, C. J., DAI, D., TRAN, K. A., MONROE, J. G. & WILLIAMS, B. P. 2023. Dynamic DNA
734 methylation turnover in gene bodies is associated with enhanced gene expression plasticity
735 in plants. *Genome Biol,* 24**,** 227.
736 ZEMACH, A., KIM, M. Y., HSIEH, P. H., COLEMAN-DERR, D., ESHED-WILLIAMS, L., THAO, K., HARMER,
737 S. L. & ZILBERMAN, D. 2013. The Arabidopsis nucleosome remodeler DDM1 allows DNA
738 methyltransferases to access H1-containing heterochromatin. *Cell,* 153**,** 193-205.
739 ZHANG, X., YAZAKI, J., SUNDARESAN, A., COKUS, S., CHAN, S. W., CHEN, H., HENDERSON, I. R., SHINN,
740 P., PELLEGRINI, M., JACOBSEN, S. E. & ECKER, J. R. 2006. Genome-wide high-resolution
741 mapping and functional analysis of DNA methylation in arabidopsis. *Cell,* 126**,** 1189-201.
742 ZHOU, H., WANG, Y., LV, Q., ZHANG, J., WANG, Q., GAO, F., HOU, H., ZHANG, H., ZHANG, W. & LI, L.
743 2016. Overexpression of Ribosomal RNA in the Development of Human Cervical Cancer Is
744 Associated with rDNA Promoter Hypomethylation. *PLoS One,* 11**,** e0163340.
745 ZILBERMAN, D., GEHRING, M., TRAN, R. K., BALLINGER, T. & HENIKOFF, S. 2007. Genome-wide
746 analysis of Arabidopsis thaliana DNA methylation uncovers an interdependence between
747 methylation and transcription. *Nat Genet,* 39**,** 61-9.

748

749

750

751 **Figure Legends**

752 **Figure 1:** Ribosomal RNA (rRNA) gene organization, subtype variation, localization and their
753 relative arrangement (A) The diagram shows a generic tandem arrangement of 45S rRNA
754 genes on a NOR. (B) The diagram shows the 3' ETS region of 45S rRNA genes that exhibit
755 length and sequence polymorphisms among the rRNA variants. (C) The gel image shows
756 HindIII CAPS assay of rRNA variants and the diagram at the bottom shows the position of
757 HindIII restriction site relative to the binding sites of primers that amplify all four rRNA
758 variants. (D) The diagram shows known locations of the rRNA variants on NOR2 and NOR4
759 in the Col-0 ecotype of *A. thaliana*.

760

761 **Figure 2**: Disruption of *NOR2* gene silencing to varying degrees in DNA methylation mutants.
762 The gel images show DNA-PCR data for rRNA gene subtypes and RT-PCR expression data
763 for rRNA gene subtypes and actin. The gel images were spliced to remove the second lane.

764

765 **Figure 3**: Methylation state of rDNA in CG, CHG, and CHH contexts. Whole genome
766 bisulfite sequencing data from various DNA methylation mutants were analyzed using
767 Methylpy, and the overall cytosine methylation state of rDNA is shown as heatmaps in all
768 three cytosine contexts. The Y-axis represents a single rDNA unit starting with a promoter
769 and ending with 3' ETS. Each line on the heatmap represents the methylation state of the
770 cytosines in a given methylation context in 50 nucleotide bins. CG is shown in red, CHG in
771 green, and CHH in blue. Grey indicates that no methylation sites were present in that bin for
772 a given context.
773 TSS= Transcription Start Site.
774
775 **Figure 4:** Cytosines in the promoters of 45S rRNA genes occur mostly in CHH, distantly
776 followed by CHG, and almost none in CG context.
777 (A) Relative distribution of cytosines among different cytosine contexts (CG, CHG, and CHH)
778 in the minimal rDNA promoter regions of different plant species. (B) For *A. thaliana* and
779 tomato, publicly available assembled NOR sequences were analyzed to quantify the number
780 of 45S rRNA gene repeats which show 100% conserved gene promoter sequence (-55 to
781 +6).
782 NA-Entire NOR sequences not available.
783
784 **Figure 5***: NOR2* genes are hypermethylated and *NOR4* genes are hypomethylated. (A) Gel
785 images on the left show resolution of HpaII- or buffer-treated Col-0 and *met1-7* DNA
786 samples, and the gel images on the right show PCR amplification of rRNA gene subtypes.
787 For these PCR reactions, gel-eluted DNA samples representing the HpaII-undigested (⩾ 20
788 kb) and the HpaII-digested (0.6-1.0 kb) fractions were used. (B) The gel images show rRNA
789 gene subtype PCR products obtained from McrBC-digested or no enzyme-treated Col-0
790 DNA.
791
792 **Figure 6**: Col-0 NOR2 genes are hypermethylated and Sf-2 NOR4 genes are
793 hypomethylated in the ColSf-NOR4 introgression line. (A) Diagram showing rRNA subtype
794 composition of the Arabidopsis introgression line called ColSf-NOR4 in which Sf-2 NOR4
795 and adjacent sequences were introgressed into the Col-0 genetic background. (B) The
796 agarose gel images on the left show resolution of HpaII- or buffer-treated ColSf-NOR4 gDNA
797 samples, and the gel images on the right show PCR amplification of rRNA variants with or
798 without HindIII digestion. For these PCR reactions, gel-eluted DNA samples representing the
799 HpaII-undigested (⩾ 20 kb) and the HpaII-digested (0.6-1.0 kb) fractions were used. (C)
800 Summary of results shown in (B). (D) The gel images show PCR amplification of rRNA

801 variants obtained from McrBC- or buffer-treated ColSf-NOR4 gDNA with or without HindIII
802 digestion. (E) Summary of results shown in (D).
803
804 **Figure 7**: Model depicting a role for CMT2-dependent CHH methylation in rRNA gene
805 silencing in *Arabidopsis*. In Wild-type, NOR2 rRNA genes are methylated in all cytosine
806 contexts. Loss of RdDM-dependent mCHH does not affect rRNA gene silencing at NOR2.
807 However, loss of CMT2-mediated mCHH results in disruption of NOR2 rRNA gene silencing
808 and likely alleviates chromatin condensation at these loci. Collectively, these findings
809 suggest that CMT2-mediated CHH methylation plays a critical role in rRNA gene silencing.
810

811 **Supplementary figure legends**

812 **Figure S1:** Disruption of NOR2 gene silencing to varying degrees in DNA methylation
813 mutants. The gel images show RT-PCR expression data for the rRNA gene subtypes and
814 actin.
815
816 **Figure S2:** The 45S rRNA gene reference sequence used to generate methylation heat
817 maps.
818
819 **Figure S3:** Occurrence of cytosines in the promoters and gene bodies of 45S rRNA genes.
820 Diagram depicting the relative distribution of cytosines in CG, CHG, and CHH contexts in the
821 promoters and gene bodies of 45S rRNA genes in (A) *Arabidopsis thaliana*, (B) tomato, and
822 in (C) human.
823
824 **Figure S4:** Primers/oligos used in this study.

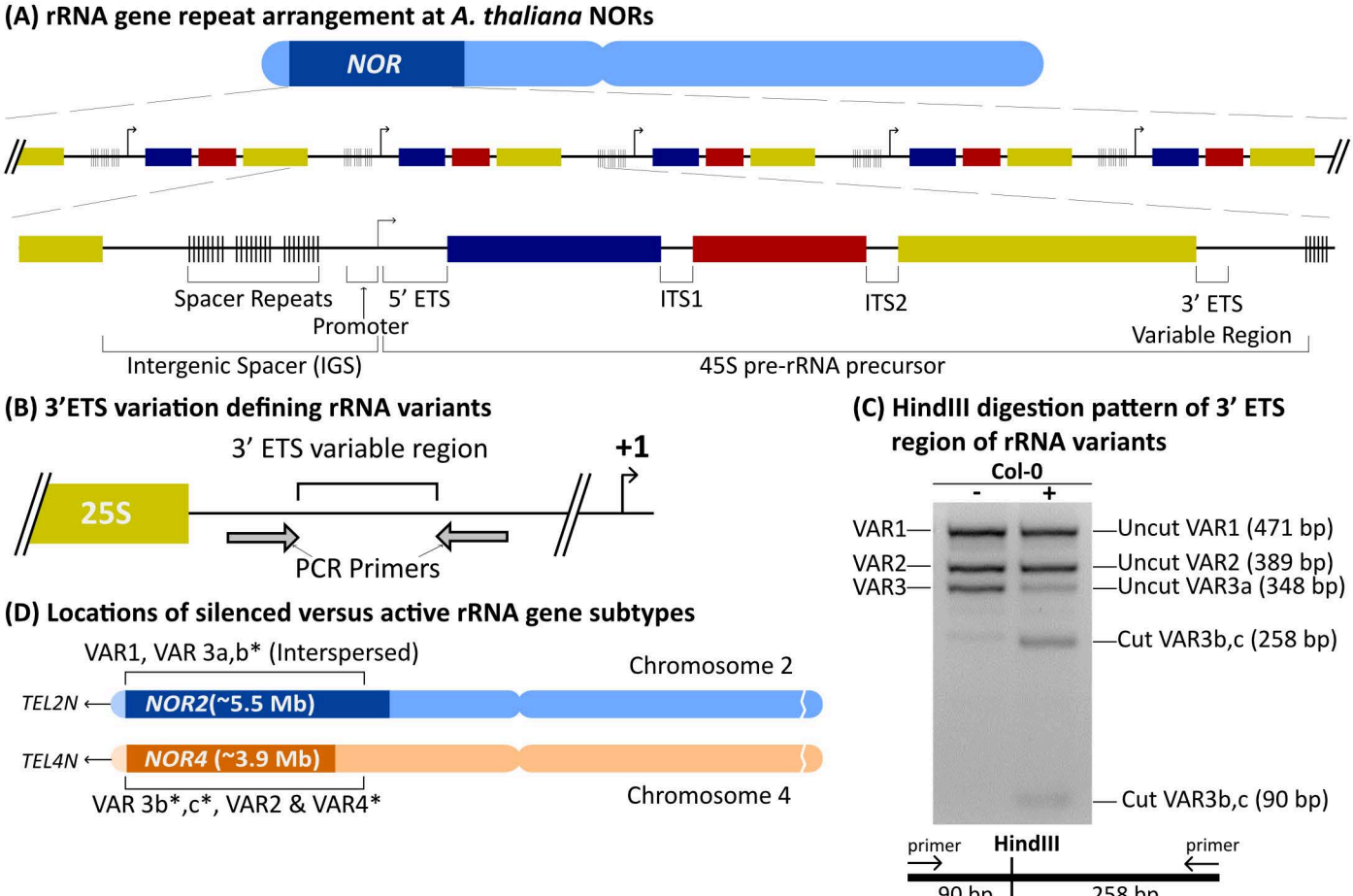

Figure 1: Ribosomal RNA (rRNA) gene organization, subtype variation, localization and their relative arrangement (A) The diagram shows a generic tandem arrangement of 45S rRNA genes on a NOR. (B) The diagram shows the 3' ETS region of 45S rRNA genes that exhibit length and sequence polymorphisms among the rRNA variants. (C) The gel image shows HindIII CAPS assay of rRNA variants and the diagram at the bottom shows the position of HindIII restriction site relative to the binding sites of primers that amplify all four rRNA variants. (D) The diagram shows known locations of the rRNA variants on NOR2 and NOR4 in the Col-0 ecotype of A. thaliana.

rRNA subtype expression in DNA methylation mutants

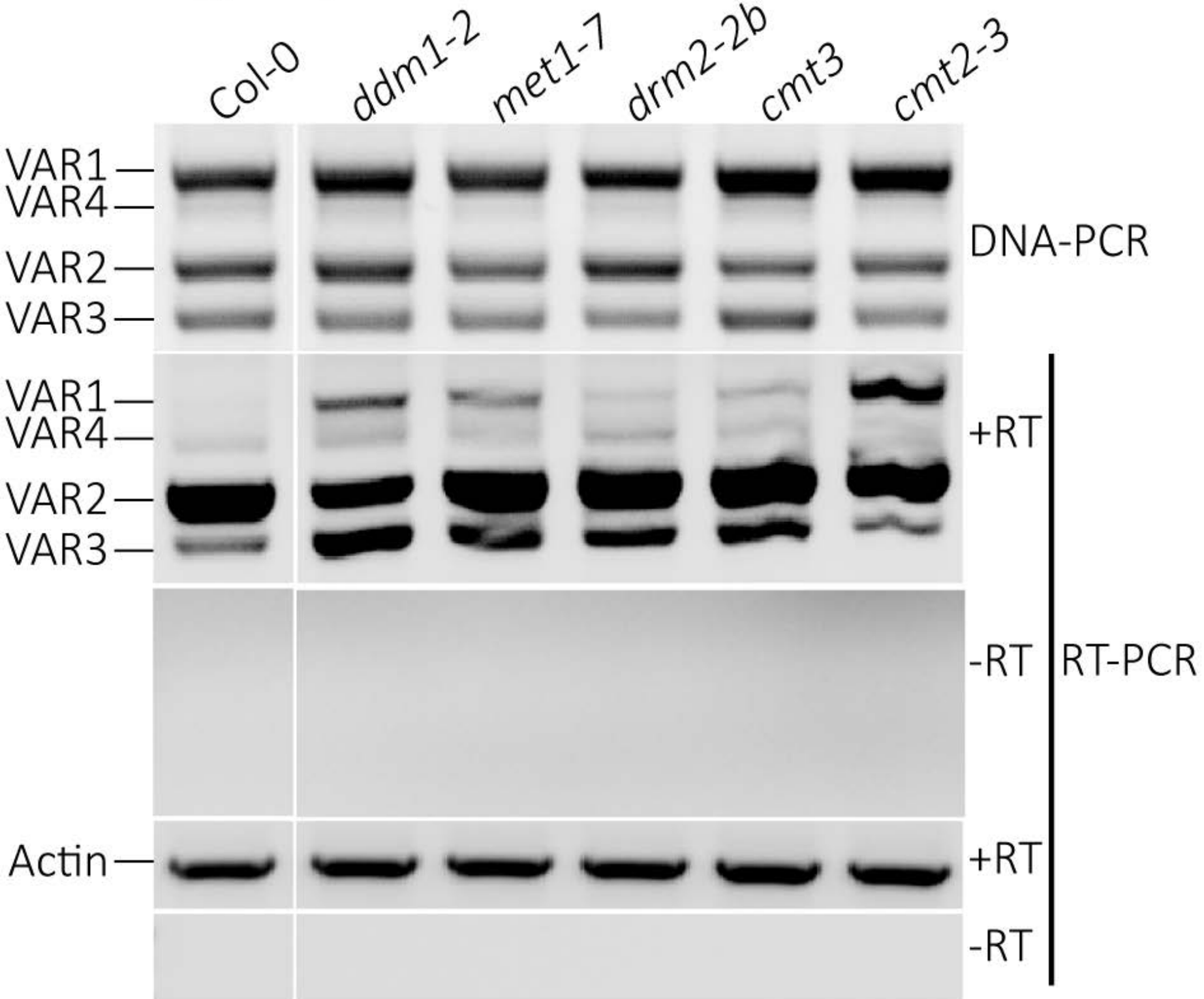

Figure 2. Disruption of *NOR2* gene silencing to varying degrees in DNA methylation mutants.

The gel images show DNA-PCR data for rRNA gene subtypes and RT-PCR expression data for rRNA gene subtypes and actin. The gel images were spliced to remove the second lane.

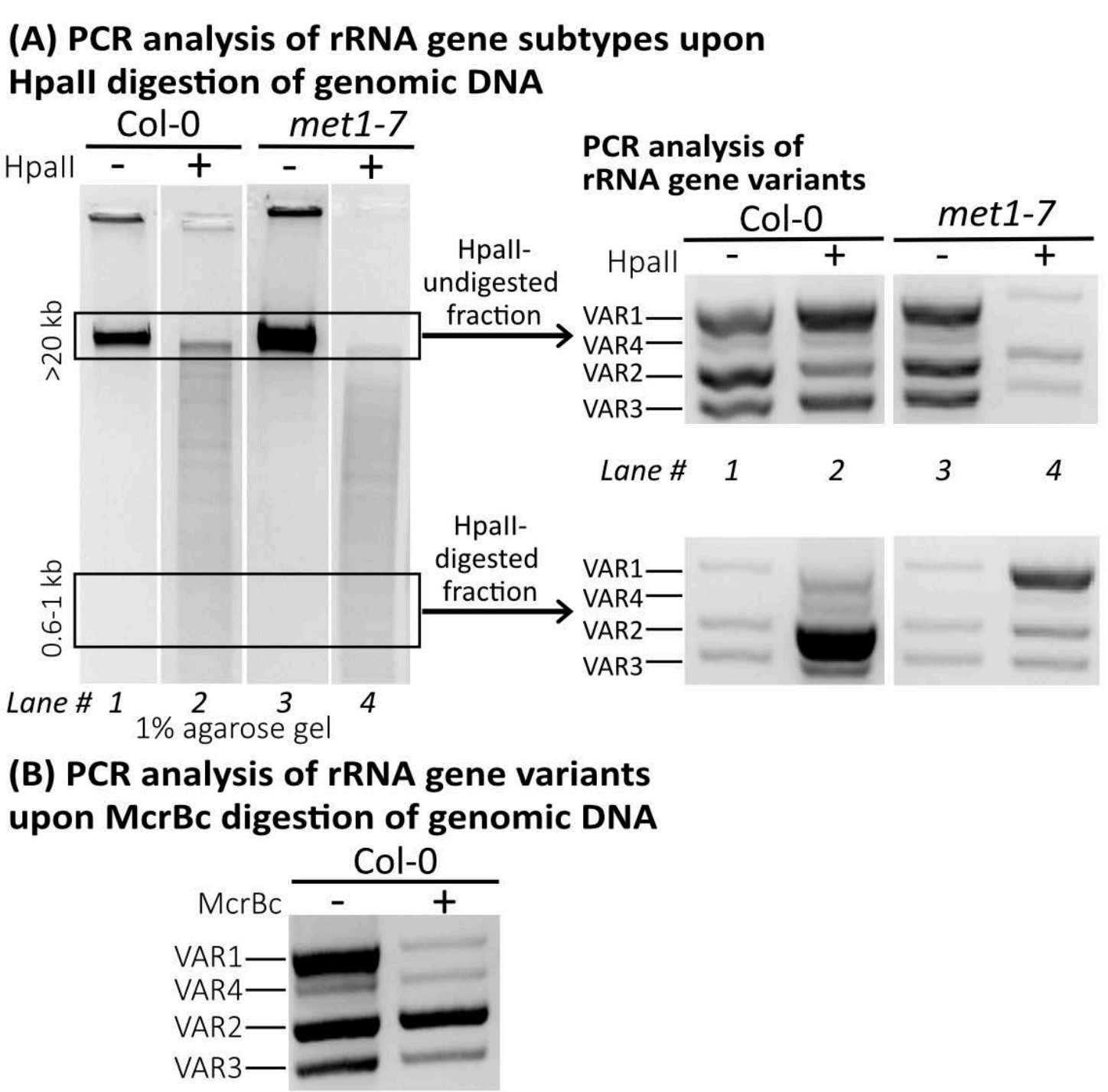

Figure 3. *NOR2* genes are hypermethylated and *NOR4* genes are hypomethylated.

(A) Gel images on the left show resolution of HpaII- or buffer-treated Col-0 and *met1-7* DNA samples and the gel images on the right show PCR amplification of rRNA gene subtypes. For these PCR reactions, gel-eluted DNA samples representing the HpaII-undigested (≥ 20 kb) and the HpaII-digested (0.6-1.0 kb) fractions were used. (B) The gel image shows rRNA gene subtype PCR products obtained from McrBc-digested or no enzyme-treated Col-0 DNA.

(A) Col$^{sf\text{-}NOR4}$ line has Col-0 *NOR2* and Sf-2 *NOR4*

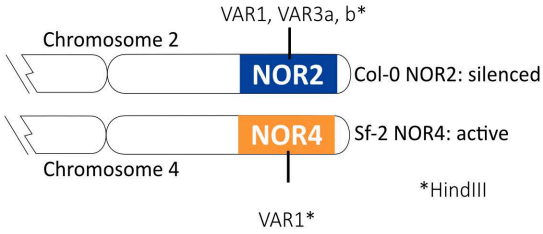

(B) HindIII CAPS analysis of rRNA gene subtypes amplified from gel-eluted fractions of HpaII-treated genomic DNA

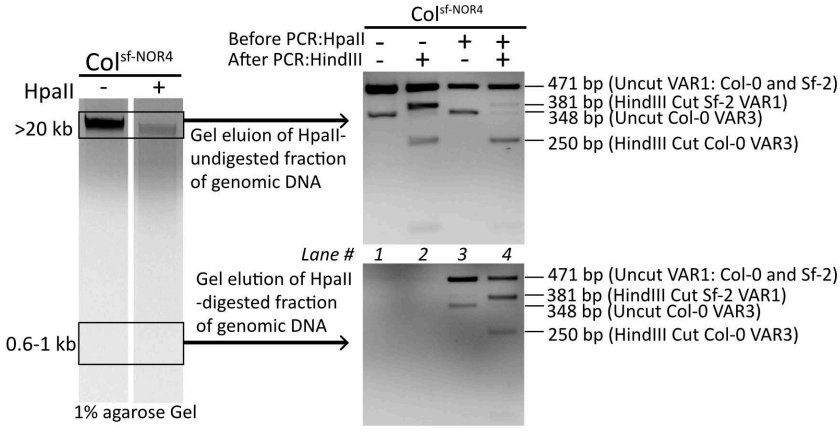

(C)

rRNA variant composition of PCR amplicons		Position of HindIII in PCR amplicons	Relative DNA methylation status	Lane 1 (no enzyme control)	Lane 2 (HindIII after PCR)	Lane 3 (HpaII before PCR & No HindIII)	Lane 4 (HpaII before PCR & HindIII after PCR)
VAR1	Sf-2 VAR1 (471 bp)	F HindIII R; 90 bp, 381 bp	hypomethylated	uncut	cut	cut by HpaII	cut by HpaII & HindIII
	Colo-0 VAR1 (471 bp)	F R	hypermethylated	uncut	uncut	uncut	uncut by HpaII or HindIII
VAR3	Col-0 VAR3a (348 bp)	F R	hypermethylated	uncut	uncut	uncut	uncut by HpaII or HindIII
	Col-0 VAR3b (348 bp)	F HindIII R; 90 bp, 258 bp	hypermethylated	uncut	cut	uncut	uncut by HpaII but cut by HindIII

F-forward primer; R-reverse primer

(D) HindIII CAPS analysis of rRNA gene subtypes amplified from McrBc-treated genomic DNA

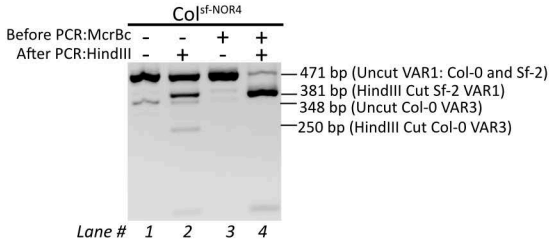

(E)

rRNA variant composition of PCR amplicons		Position of HindIII in PCR amplicons	Relative DNA methylation status	Lane 1 (no enzyme control)	Lane 2 (HindIII after PCR)	Lane 3 (McrBc before PCR & No HindIII)	Lane 4 (HpaII before PCR & HindIII after PCR)
VAR1	Sf-2 VAR1 (471 bp)	F HindIII R; 90 bp; 381 bp	hypomethylated	uncut	cut	uncut	uncut by McrBc & cut by HindIII
VAR1	Colo-0 VAR1 (471 bp)	F R	hypermethylated	uncut	uncut	cut by McrBc	cut by McrBc & uncut by HindIII
VAR3	Col-0 VAR3a (348 bp)	F R	hypermethylated	uncut	uncut	cut by McrBc	cut by McrBc & uncut by HindIII
VAR3	Col-0 VAR3b (348 bp)	F HindIII R; 90 bp; 258 bp	hypermethylated	uncut	cut	cut by McrBc	cut by McrBc & HindIII

F-forward primer; R-reverse primer

Figure 4. Col-0 *NOR2* genes are hypermethylated and Sf-2 *NOR4* genes are hypomethylated in the Col$^{sf\text{-}NOR4}$ introgression line. (A) Diagram showing rRNA subtype composition of the Arabidopsis introgression line called Col$^{Sf\text{-}NOR4}$ in which Sf-2 *NOR4* and adjacent sequences were introgressed into the Col-0 genetic background. (B) The agarose gel images on the left show resolution of HpaII- or buffer-treated Col$^{sf\text{-}NOR4}$ gDNA samples, and the gel images on the right show PCR amplification of rRNA variants with or without HindIII digestion. For these PCR reactions, gel-eluted DNA samples representing the HpaII-undigested (≥ 20 kb) and the HpaII-digested (0.6-1.0 kb) fractions were used. (C) Summay of results shown in (B). (D) The Gel image shows PCR amplification of rRNA variants obtained from McrBc- or buffer-treated Col$^{Sf\text{-}NOR4}$ gDNA with or without HindIII digestion. (E) Summary of results shown in (D).

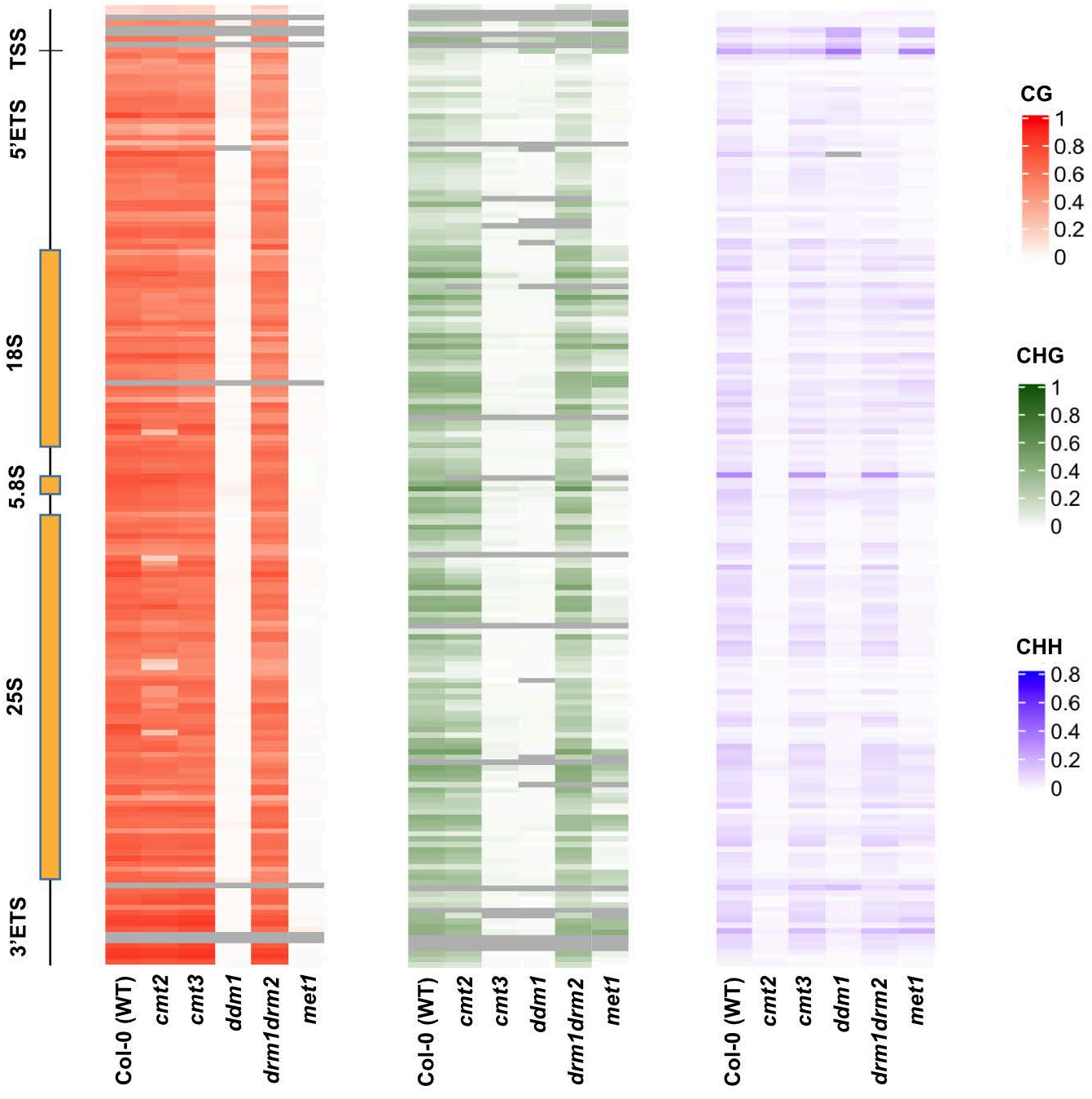

Figure 5: Methylation state of rDNA in CG, CHG, and CHH contexts. Whole genome bisulfite sequencing data from various DNA methylation mutants were analyzed using Methylpy, and the overall cytosine methylation state of rDNA is shown as heatmaps in all three cytosine contexts. The Y-axis represents a single rDNA unit starting with a promoter and ending with 3' ETS. Each line on the heatmap represents the methylation state of the cytosines in a given methylation context in 50 nucleotide bins. CG is shown in red, CHG in green, and CHH in blue. Grey indicates that no methylation sites were present in that bin for a given context. TSS= Transcription Start Site

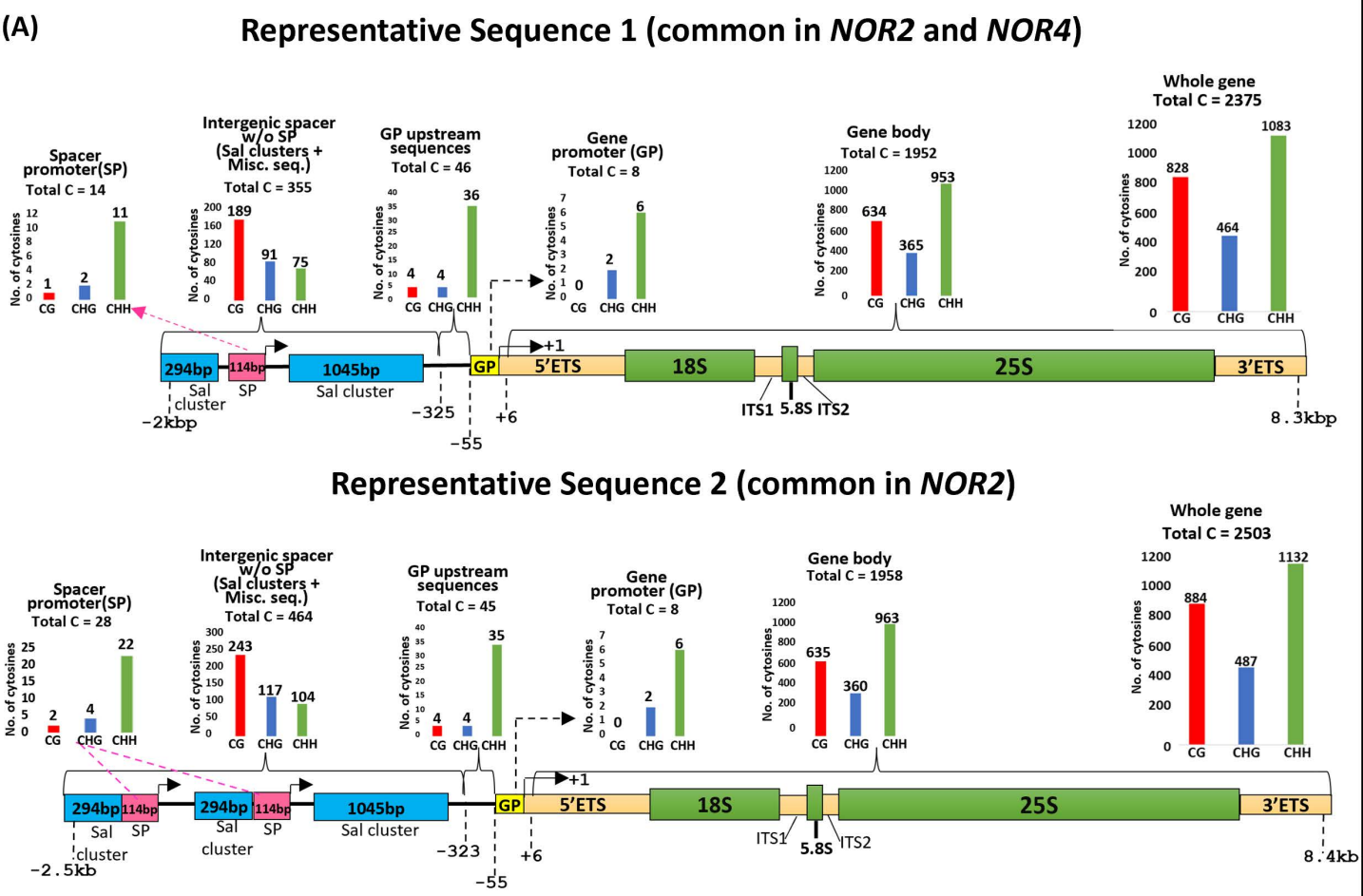

(B)

45S rRNA minimal gene promoter

-55 -20 +1

		Reference
A. thaliana	TCAGACATTTCAATGTCTGTTGGTGCCAAGAGGGAAAAGGGCTATTAAGCTATATAGGGGG	Doelling & Pikaard, 1995
Tomato	CTGGAAAATCCATGTCTACTCCTGTCACATGGGCAAAACTTTTTTAAGCATATATAAGGGG	Doelling & Pikaard, 1995; Shirasawa & Ariizumi, 2024
Radish	GGAACAGAACAATGTCGACTTGGTGAAAGACTGAAAAAAAGCTTAAGTGTTATATAGGGGG	Doelling & Pikaard, 1995
Pea	AGGGAAAAAGGGACCCAGTTGCTGCTAAAGCAGGACATGCAAATCAAGCTTATATAGGGGG	Doelling & Pikaard, 1995
Cucumber	CGGAAATTTCATATGCAAGCCTGCCAGACCAAAAAAAGTCCAAAATGTACTATATAGGGGG	Doelling & Pikaard, 1995
N. benthamiana	CTCTGACAAAGCATGTCTACTCCTGAAATTTGGGTTTTTTTTTTTAAGTATATATAAGGGG	https://solgenomics.net/

(C)

	Total C	CG	CHG	CHH	Number of 45S rRNA gene repeats with conserved gene promoter sequence	Reference
A. thaliana	8	0	2	6	Total: 859 (out of 894) (*NOR2*: 509/518, *NOR4*: 350/376)	Doelling & Pikaard, 1995 Fultz et al., 2023
Tomato	12	0	2	10	*NOR2*: 1473/1500	Shirasawa & Ariizumi, 2024
Radish	6	1	2	3	NA	Doelling & Pikaard, 1995
Pea	10	0	3	7	NA	Doelling & Pikaard, 1995
Cucumber	12	1	2	9	NA	Doelling & Pikaard, 1995
N. benthamiana	8	0	2	6	NA	https://solgenomics.net/

Figure 6. Within the 45S rRNA genes, cytosine occurrence is the highest in CHH context, followed by CG, and the lowest in CHG context. (A) A diagram provides cytosine distribution within different regions of 45S rRNA gene sequences. Based on the NOR sequences from Fultz et al., 2023, two reference sequences are chosen for representation based on their common occurrence in NORs **(B)** Sequences show relative distribution of cytosines among different cytosine contexts (CG, CHG, and CHH) in the minimal rRNA gene promoter (GP) regions of different plant species. **(C)** A table shows the number of cytosines in different sequence contexts across different plant species. For *A. thaliana* and tomato, data were obtained from Fultz et al., 2023 and Shirasawa and Ariizumi, 2024, respectively, while the data for other species were obtained from Doelling & Pikaard, 1995.

NA-Entire NOR sequences not available.

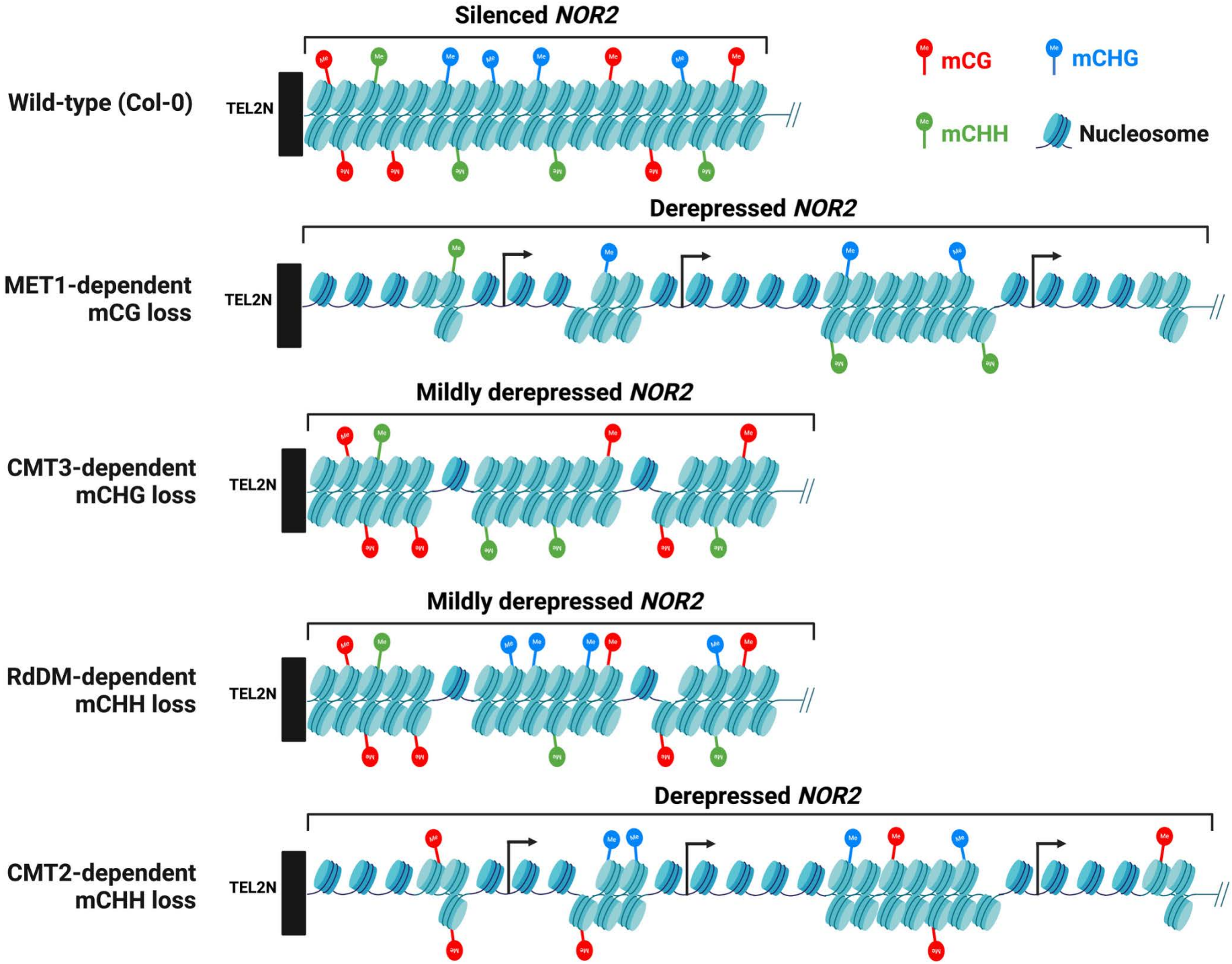

Figure 7. Model depicting a role for CMT2-dependent CHH methylation and other cytosine methylation pathways in rRNA gene silencing in Arabidopsis.

In Wild-type Col-0, *NOR2* rRNA genes are methylated in all cytosine contexts. Loss of CMT2-mediated mCHH or MET1-mediated mCG results in significant disruption of *NOR2* rRNA gene silencing and likely alleviates chromatin condensation at these loci. However, loss of CMT3-dependent mCHG or RdDM-dependent mCHH has a mild effect on rRNA gene silencing release at *NOR2*. The model takes into account the levels of NOR2 gene silencing disruption (Fig. 2) and the levels of cytosine methylation loss at each context (Fig. 3) for each of the cytosine methylation pathway mutants.